

# Crystallography-guided characterization of novel cytosolic DNase 3' repair exonuclease 1 (TREX1) inhibitors

Valerie Chen, David Hsieh, Dave Freund, Anja Holtz, Jesus Garcia Lopez, Alyssa Mullenix, Jamie Cope, Peppi Prasit, Anne Moon, Nathan Standifer, Thomas Dubensky, Henry Johnson, Dara Burdette, and Sam Whiting

Tempest Therapeutics, Brisbane, CA

## BACKGROUND

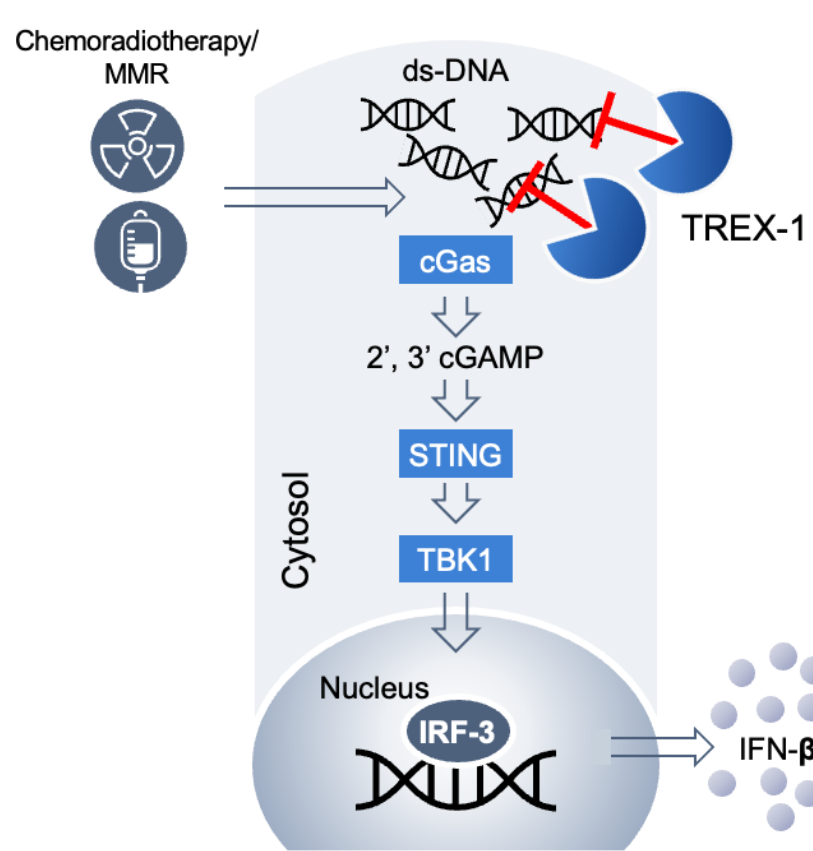


Figure 1. TREX1 controls activation of STING

### Stimulator of Interferon Genes (STING)

- Cyclic GMP-AMP synthase (cGAS) is an innate immune sensor that can activate STING in response to cytosolic double-stranded DNA (dsDNA) that accumulates in tumor cells<sup>1,2</sup>
- Functions as a critical checkpoint in immune response to tumors, inducing CD8<sup>+</sup> T cell priming against unique antigenic footprints and reversing the immunosuppressive tumor microenvironment in advanced cancers<sup>3,4</sup>
- Significant role in tumor development; inactivated in some cancers, promoting immune escape<sup>5-8</sup>
- Validated target for cancer therapeutics with several promising clinical stage STING agonists, but achievement of therapeutic index is limited due to its ubiquitous expression, as well as poor pharmacokinetics (PK) and bioavailability<sup>7,8</sup>

### OBJECTIVE

To characterize the physicochemical, *in vitro*, and *in vivo* properties of rationally-designed, small molecule TREX1 inhibitors that were optimized using a structure-based design strategy

### 3' Repair Exonuclease 1 (TREX1)

- Cytosolic exonuclease repair protein that degrades cytosolic dsDNA, downregulating the activation of cGAS/STING<sup>9,10</sup>
  - Upregulated in the tumor microenvironment in response to<sup>10</sup>:
    - Genetic instability
    - Inflammation
    - DNA replication
    - Therapeutic intervention (e.g., cytotoxic therapy, radiotherapy)
  - Failure to degrade dsDNA (e.g., through TREX1 inhibition) activates the cGAS-STING pathway and promotes interferon-dependent antitumor immunity<sup>8,9</sup>
- ### TREX1 Inhibition as a Therapeutic Approach for Cancer
- By leveraging the role of TREX1 as the main gatekeeper in the cGAS/STING signaling pathway, small molecule TREX1 inhibitors were rationally designed using a structure-based drug design strategy to drive robust anti-tumor immunity
  - TREX1 inhibition is hypothesized to selectively activate STING in the TME, providing an approach to broadly activate innate immune signaling in metastatic disease

## METHODS

### In Vitro Assays for TREX1 Inhibitor Activity

- Recombinant TREX1 Nuclease Assay:** Truncated TREX1 recombinant protein encompassing the catalytic domain (residues 2-242) was incubated with compounds and a double-stranded DNA substrate was added to initiate the nuclease reaction. Double-stranded DNA remaining at specific time points were quantified by PicoGreen fluorescence.
- Lysate TREX1 Nuclease Assay:** Cytosolic lysates from CT26 or THP1 cells expressing endogenous, full-length TREX1 were incubated with compound. A double-stranded DNA substrate covalently-modified with a 5' fluorophore on the sense strand and 3' fluorescence quencher on the antisense strand was added to initiate the nuclease reaction. TREX1 nuclease activity can be quantified by measuring fluorescence intensity over time.
- Cellular Reporter Assay:** HCT116 cells were treated with compound for 4 hours at 37°C, followed by transfection with BstNI-digested pBR322. DNA-stimulated cells were then incubated at 37°C for an additional 48 hours before monitoring for IRF3 reporter luciferase activity. Luciferase reporter activity with compound treatment was compared to DNA-stimulation alone.

### In Vivo Studies in Tumor Models

- Anti-tumor Activity in Lymphoma Model:** Groups of 10 B6 mice were implanted with EG7.OVA tumor cells on D0. At tumor size of 80 mm<sup>3</sup>, tumors were given 10 μg of doxorubicin intratumorally and/or treated with compound 4A at 75 mg/kg intraperitoneally BID for 14 days. Tumor growth and body weight were measured every 3 days
- Pharmacodynamic (PD) Analysis:** Tumor lysates were prepared from compound 4A- and vehicle-treated animals for *ex vivo* nuclease assays. Nuclease activity for each tumor was measured as fluorescence intensity over time and compared to vehicle-treated nuclease activity
- Pharmacokinetic (PK) Analysis:** Compound 4A was administered to B6 mice at 75 mg/kg intraperitoneally BID for 14 days. On day 14 tumor samples were collected at 15 min, 4 h, and 24 h. Concentrations of compound 4A was measured by LC-MS/MS

## RESULTS

### Developing a First-in-Class TREX1 Inhibitor Using Co-crystal Structures of Inhibitor-Bound TREX1

- Human TREX1 inhibitor Target Candidate Profile (TCP) shows desirable properties for potent and selective TREX1 inhibitors (Table 1)

Table 1. Human TREX1 inhibitor Target Candidate Profile (TCP)

		Lead Molecule
Biochemical Potency	Human PicoGreen dsDNA Assay (nM)	≤ 10 nM IC <sub>50</sub>
Cellular Potency (IFN-β)	THP1, HCT116, or other (nM)	< 1 μM EC <sub>50</sub>
Selectivity	Toxicity/Specificity	CC <sub>50</sub> > EC <sub>50</sub> in cellular assays
Physicochemical Properties	MW / cLogD	< 500 / < 4
Pharmacokinetics	Rodent PK	% F > 30 Low-Moderate Clearance

- Co-crystal structures of human TREX1 in complex with first-in-class TREX1 inhibitors confirm Mg<sup>2+</sup>-dependent mechanism of inhibition (Figure 2)

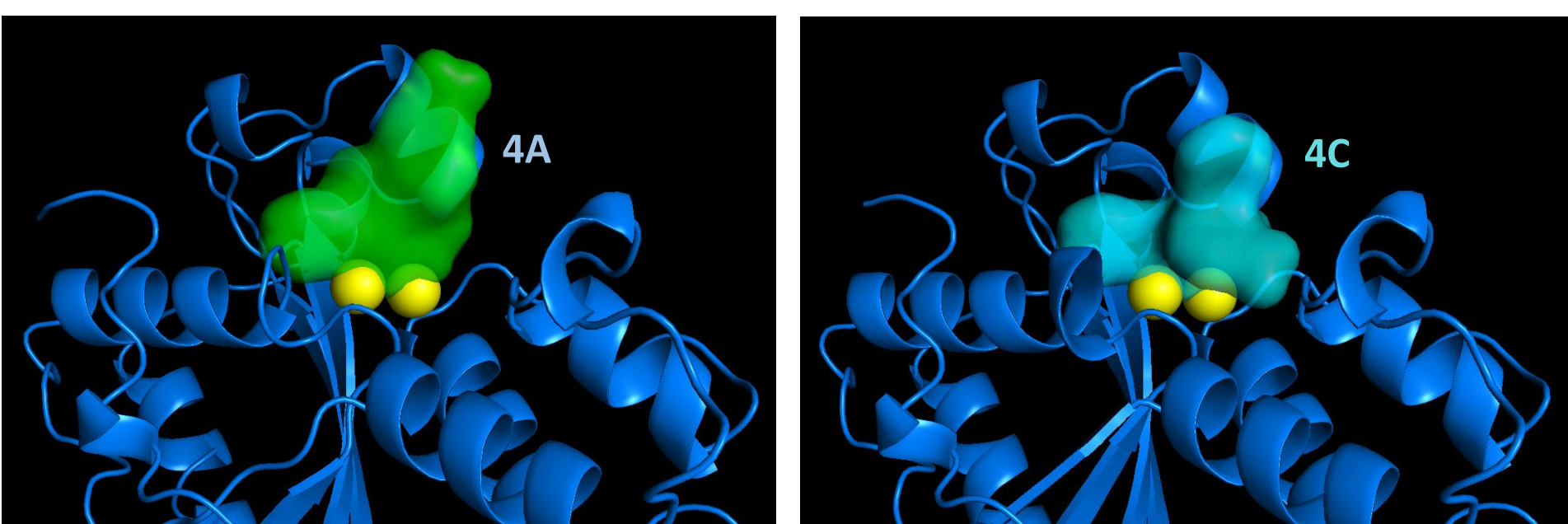


Figure 2. X-ray co-crystal structure of human TREX1 in complex with Compound 4A and 4C. X-ray co-crystal structures of human TREX1 (blue) in complex with inhibitors (green, cyan) confirm Mg<sup>2+</sup>-dependent mechanism of inhibition. The two catalytic Mg<sup>2+</sup> ions in the active site are shown in yellow. Crystallized human TREX1 is a human to mouse chimera containing the following point mutations: A5T, P8H, P10H.<sup>11</sup> The previously published human TREX1 crystal structures lack the two catalytic Mg<sup>2+</sup> ions in the active site.

### Biophysical Characterization of Recombinant TREX1 with Compound 4A by SPR and TSA

- Single-cycle kinetics surface plasmon resonance (SPR) analysis with site-specifically biotinylated human and mouse TREX1 (2-242) showed nanomolar binding affinity of human and mouse TREX1 for Compound 4A (Figure 3A)
- Thermal shift analysis (TSA) with and without MgCl<sub>2</sub> confirmed a Mg<sup>2+</sup>-ion-dependent mode of binding for Compound 4A (Figure 3B); MgCl<sub>2</sub> also enhanced the thermal stability of the TREX1 recombinant protein

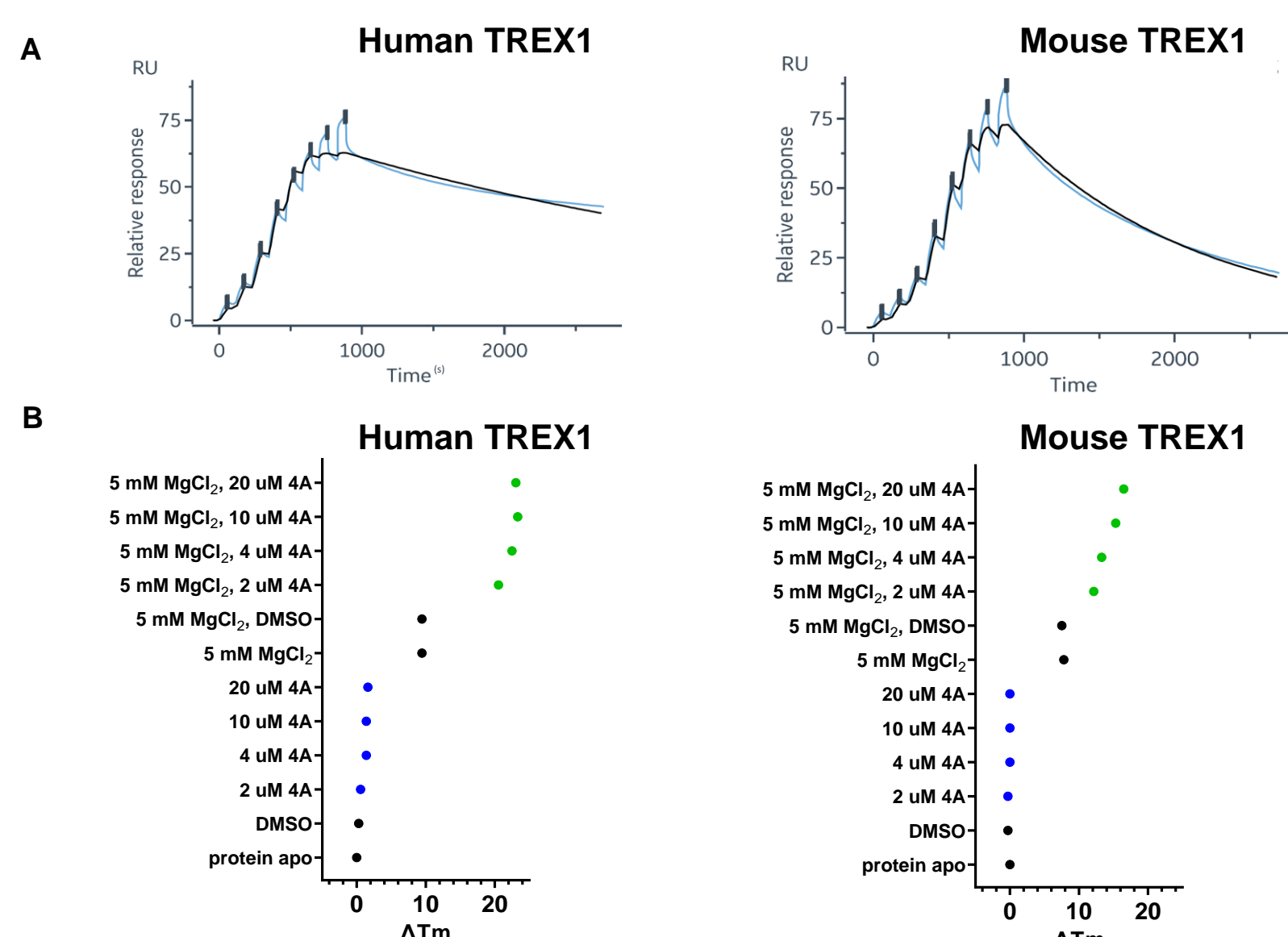


Figure 3. Surface plasmon resonance and thermal shift analysis for Compound 4A using human and mouse TREX1 (2-242) recombinant proteins. (A) Single-cycle kinetics SPR analysis with site-specifically biotinylated human and mouse TREX1 (2-242). (B) Thermal shift analysis with (green) and without (blue) MgCl<sub>2</sub>

- Human recombinant TREX1 had a lower K<sub>D</sub> and a longer residence time than its mouse counterpart (Table 2)

Table 2. K<sub>D</sub> and residence time of Compound 4A complex with human vs. mouse TREX1 recombinant proteins

Species	K <sub>D</sub> (nM)	Residence time (min)
Human	78	67
Mouse	414	21

### Elucidating Human and Mouse Species Specificity of TREX1 Inhibitors with Crystal Structures

- High resolution co-crystal structures of human and mouse TREX1 in complex with TREX1 inhibitors and catalytic Mg<sup>2+</sup> ions were used to determine mouse- and human-specific interactions, identifying key residues of TREX1 that drive species specificity (Figure 4A)
- Enzymatic assays demonstrated that TREX1 inhibitors were more potent against human TREX1 than mouse TREX1 (Figure 4B)
- Human and mouse TREX1 chimeras were produced with swapped species-specific active site residues to determine key residues in each species that increase or decrease potency of candidate TREX1 inhibitors (Figure 4C)

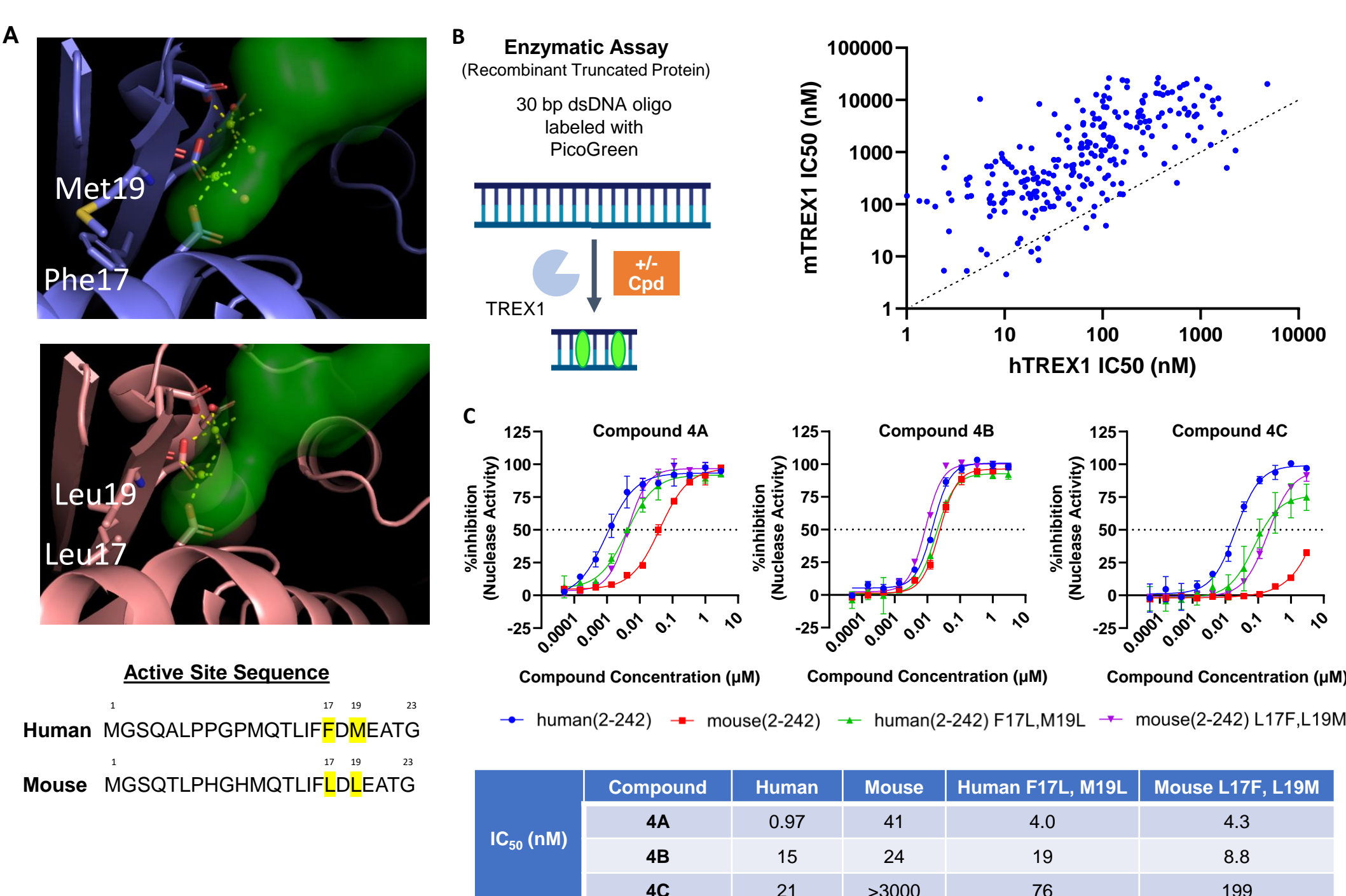


Figure 4. Active site chimeras reveal two residues are responsible for human/mouse interspecies potency differences of TREX1 inhibitors. (A) Human TREX1 (blue) and mouse TREX1 (pink) bound to compound 4A (green). The two Mg<sup>2+</sup> ions in the active site are coordinated by waters, acidic side chains (D18, E20, D130, and D200), compound 4A, and the backbone carbonyl of residue 19. Active site-adjacent N-terminal sequence differences between human and mouse TREX1 are highlighted in yellow. (B) Scatterplot comparing human and mouse enzymatic IC<sub>50</sub> values show that TREX1 inhibitors are more potent against human TREX1 with a potency difference of ~15X. (C) Active site human and mouse TREX1 chimeras were tested with two compounds with decreased mouse potency (4A and 4C) and an equipotent compound (4B). Active site chimeras have intermediate IC<sub>50</sub> values for compounds 4A and 4C when compared to WT human and WT mouse proteins. Data are shown as mean ± SD

### Nuclease Activity and STING Activation by Compound 4A

- Compound 4A demonstrated nanomolar potency in inhibiting TREX1 nuclease activity in the cytoplasmic fraction of THP1 and CT26 cell lysates (Figure 5) and increased STING activation in a cellular reporter assay (Figure 6)

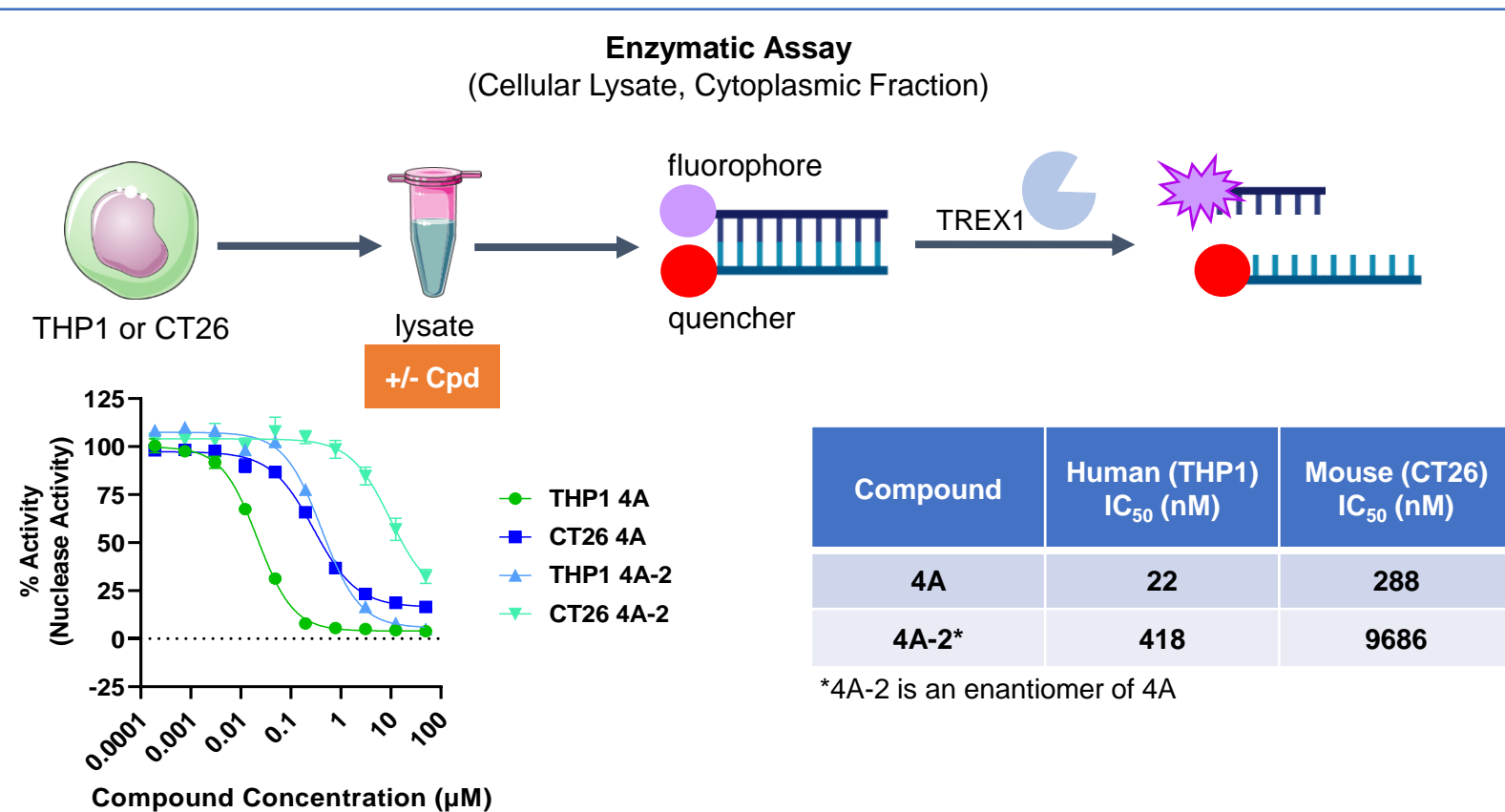


Figure 5. Compound 4A inhibits TREX1 nuclease activity from both CT26 and THP1 cytoplasmic lysates. Negligible non-TREX1 nuclease activity was detected from CT26 and THP1 TREX1 knockout lysates (data not shown). Data are shown as mean ± standard deviation (SD)

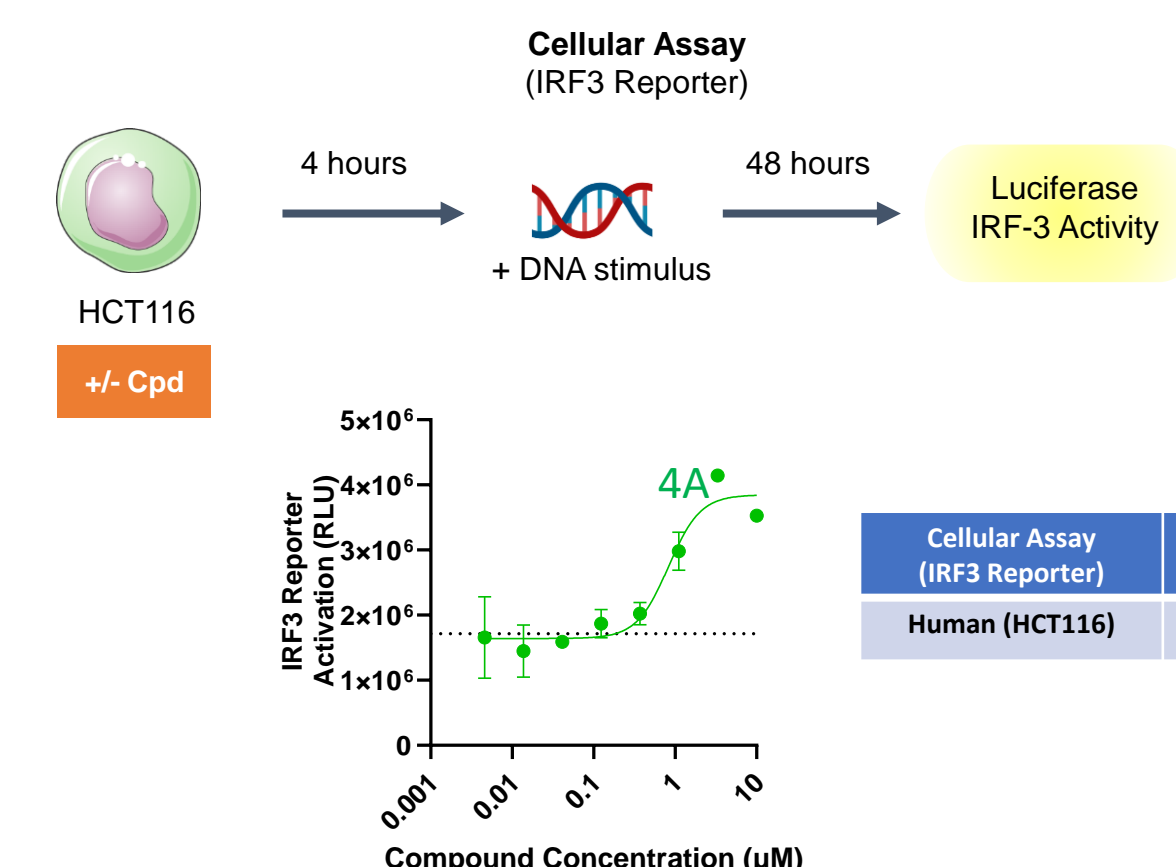


Figure 6. Compound 4A increases STING activation in DNA-stimulated HCT116 IRF3 reporter cells. No IRF3 reporter activity above DNA alone was detected in HCT116 TREX1 knock out reporter cells with compound 4A treatment (data not shown) confirming that enhanced IRF3 signaling after compound 4A treatment is a TREX1-dependent effect. Data are shown as mean ± SD

### Anti-Tumor Activity and PK/PD Analysis in Murine Models

- Administration of Compound 4A alone or in combination with doxorubicin significantly reduced tumor volumes in mice implanted with CT26 tumor cells, compared with vehicle only (Figure 7), and PK/PD relationship confirmed target engagement in tumors (Figure 8)

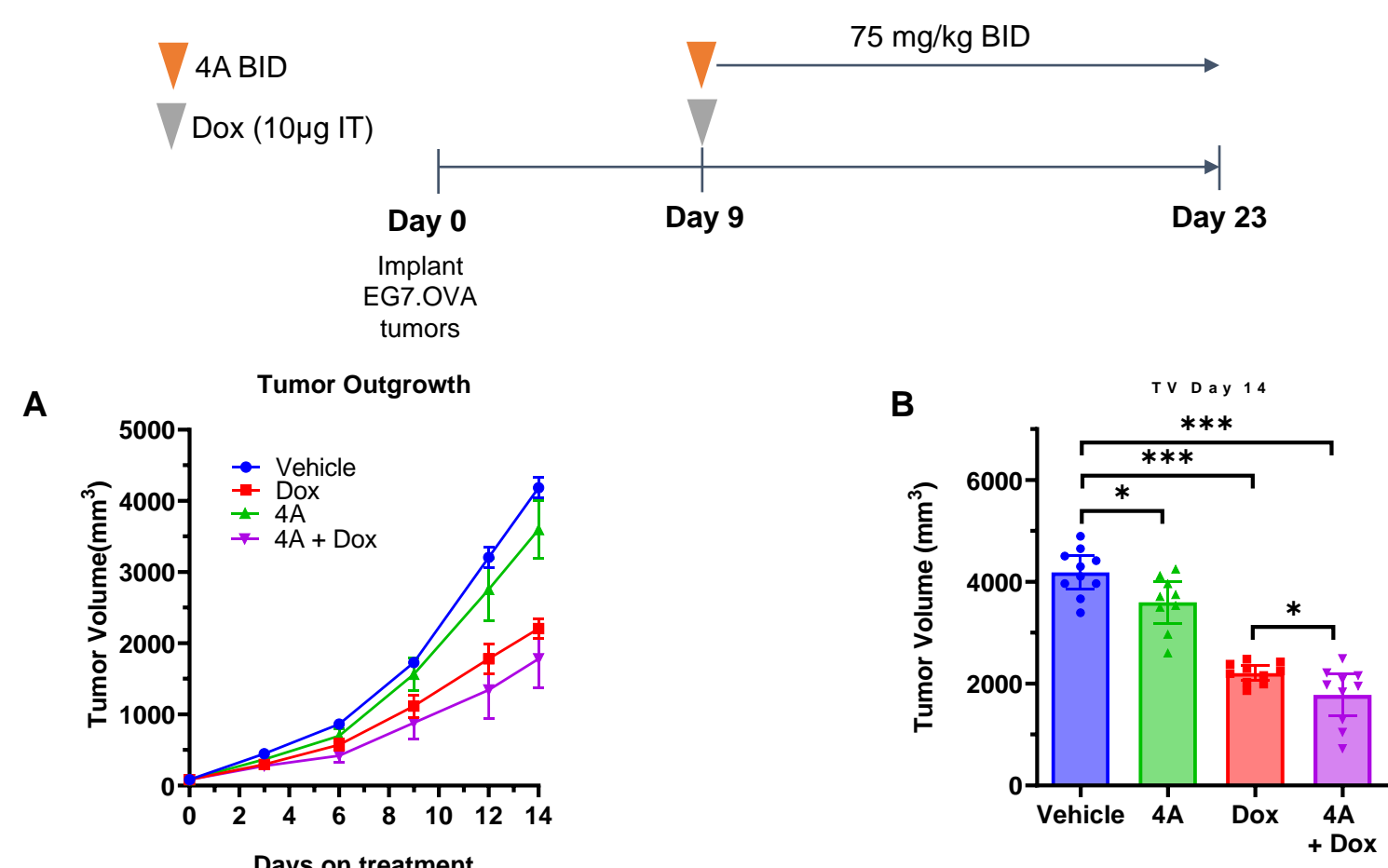


Figure 7. Compound 4A inhibition of TREX1 activity results in anti-tumor activity when combined with low-doses of doxorubicin (Dox). (A) Tumor volume over time. Data are shown as mean ± SEM. Body weights demonstrated no additive toxicity with doxorubicin (data not shown). (B) Tumor growth at D14. Unpaired 2-sided T-test revealed significantly reduced tumor volumes in groups as shown. \*P < 0.05; \*\*\*P < 0.0001

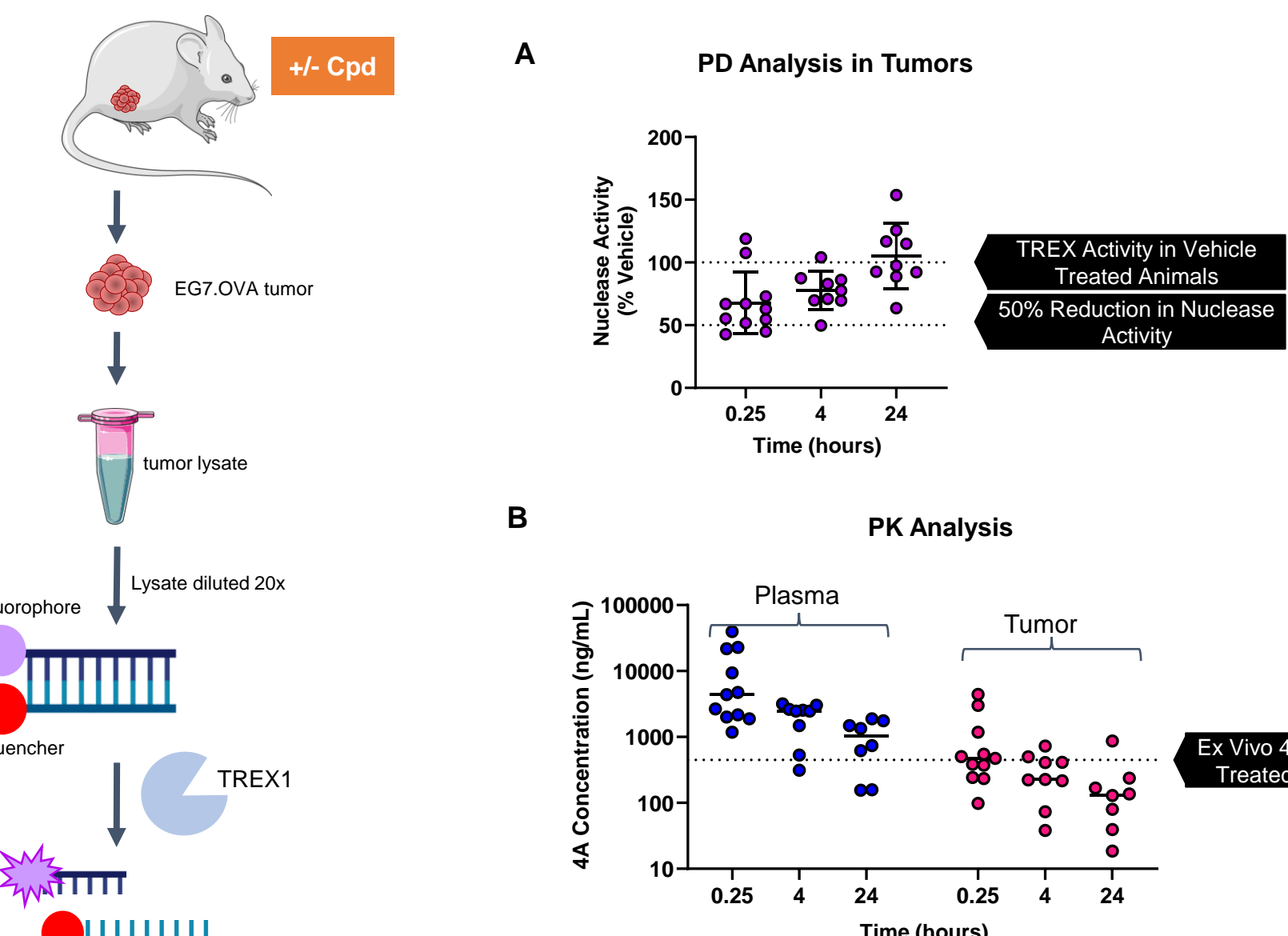


Figure 8. Pharmacokinetic/pharmacodynamic relationship confirms target engagement in tumors. (A) Pharmacodynamic analysis in tumors. (B) Pharmacokinetic profile of compound 4A. The dotted line represents the nuclease activity EC<sub>50</sub> value of compound 4A spiked into vehicle-treated tumor lysates

## CONCLUSIONS & FUTURE DIRECTIONS

- A series of novel first-in-class TREX1-specific inhibitors was designed and characterized with nanomolar potency against human and mouse TREX1
- Crystal structures of human and mouse TREX1 in complex with TREX1 inhibitors and catalytic Mg<sup>2+</sup> ions were used to determine mouse- and human-specific interactions, enabling identification of key residues of TREX1 that drive species specificity
- TREX1 inhibition with compound 4A inhibited nuclease activity, activated STING *in vitro*, and elicited anti-tumor activity *in vivo*, both alone and in combination with doxorubicin
- Our findings suggest that TREX1 inhibition with compound 4A engages the STING pathway in the tumor microenvironment, enhances tumor-specific immunity, and has potential to provide therapeutic benefit in a clinical setting

REFERENCES: 1. Sun L, et al. Science. 2013;339:786-91; 2. Wu J, et al. Science. 2013;339:826-30; 3. Woo SR, et al. Immunity. 2014;41:830-42; 4. Demaria O, et al. PNAS. 2015;112:15408-13; 5. An X, et al. Mol Ther Nucleic Acids. 2018;14:80-9; 6. Lemos H, et al. Cancer Res. 2016;76:2076-81; 7. Zhu Y, et al. Mol Cancer. 2019;18:152; 8. Gan Y, et al. Frontiers Immunol. 2021;12:795401; 9. Hemphill WO, et al. Frontiers Immunol. 2021;12:660184; 10. Simpson SR, et al. DNA Repair. 2020;94:102894; 11. Zhou W, et al. Nature Communications. 2022; 10.1038

ACKNOWLEDGMENTS: Ingrid Koo, PhD, provided editorial support for the poster.